


Extracellular Vesicle Proteome of Breast Cancer Patients with and Without Cognitive Impairment Following Anthracycline-based Chemotherapy: An Exploratory Study

Biomarker Insights
Volume 16: 1–12
© The Author(s) 2021
Article reuse guidelines:
sagepub.com/journals-permissions
DOI: 10.1177/11772719211018204



Yong Qin Koh¹, Ding Quan Ng² , Chiu Chin Ng¹, Adrian Boey¹, Meng Wei³, Siu Kwan Sze³, Han Kiat Ho¹, Munjal Acharya⁴, Charles L Limoli⁴ and Alexandre Chan^{2,5}

¹Department of Pharmacy, Faculty of Science, National University of Singapore, Singapore.

²Department of Clinical Pharmacy Practice, University of California, Irvine, CA, USA. ³School of Biological Sciences, Nanyang Technological University, Singapore. ⁴Department of Radiation Oncology, University of California, Irvine, CA, USA. ⁵Department of Oncology Pharmacy, National Cancer Centre Singapore, Singapore.

ABSTRACT: Cognitive impairment due to cancer and its therapy is a major concern among cancer patients and survivors. Extracellular vesicle (EVs) composition altered by cancer and chemotherapy may affect neurological processes such as neuroplasticity, potentially impacting the cognitive abilities of cancer patients and survivors. We investigated the EV proteome of breast cancer patients with and without cognitive impairment following anthracycline-based chemotherapy from longitudinally collected plasma. EVs were cup-shaped and positive for Flotillin-1 and TSG-101. We identified 517 differentially expressed EV proteins between the cognitive impaired and non-impaired groups during and post-chemotherapy. The observed decreased expression of p2X purinoceptor, cofilin-1, ADAM 10, and dynamin-1 in the plasma EVs of the cognitive impaired group may suggest alterations in the mechanisms underlying synaptic plasticity. The reduced expression of tight junction proteins among cognitive-impaired patients may imply weakening of the blood-brain barrier. These EV protein signatures may serve as a fingerprint that underscores the mechanisms underlying cognitive impairment in cancer patients and survivors.

KEYWORDS: Extracellular vesicles, cancer, chemotherapy, cancer-related cognitive impairment, mass spectrometry

RECEIVED: November 2, 2020. **ACCEPTED:** April 27, 2021.

TYPE: Original Research

FUNDING: The author(s) disclosed receipt of the following financial support for the research, authorship, and/or publication of this article: This work was supported by research funding and grants awarded by National Medical Research Council Grant Singapore (NMRC/CIRG/1386/2014 and NMRC/CIRG/1471/2017; principal investigator Dr. Alexandre Chan).

DECLARATION OF CONFLICTING INTERESTS: The author(s) declared no potential conflicts of interest with respect to the research, authorship, and/or publication of this article.

CORRESPONDING AUTHOR: Alexandre Chan, 147B Bison Modular, Department of Clinical Pharmacy Practice, University of California, Irvine, CA 92697, USA. Email: a.chan@uci.edu.

Introduction

Cancer and chemotherapy-related cognitive impairment (CRCI) is increasingly recognized as a critical concern for cancer survivors.^{1,2} Among breast cancer patients, anthracycline-based therapies are widely used and have consistently been reported to cause CRCI.³ In our previous study, we have observed that approximately half of the breast cancer patients receiving chemotherapy reported cognitive impairments during and post-treatment, and up to one-third experienced deficits at 15 months post-treatment.⁴ Affected patients experienced difficulty resuming pre-cancer responsibilities and activities, which could negatively impact their quality of life.^{5,6} In managing CRCI, non-pharmacological interventions such as physical activity⁷ and cognitive rehabilitative program⁸ were shown to improve patients' psychosocial functioning and neurocognitive performance. However, effective pharmacological treatments for CRCI short- and long-term after cessation of cancer therapy are lacking in view of the poor understanding of the underlying pathophysiology.

Extracellular vesicles (EVs) are cell-secreted spherical vesicles surrounded by a lipid bilayer, between 30 and 1000 nm in diameter.⁹ The pathways leading to EV biogenesis results in EVs expressing surface markers reflecting their cellular origin.¹⁰

Cells selectively sort bioactive molecules (eg, proteins and microRNAs) into EVs, protects them from enzymatic degradation, and transport its cargo into targeted cells to regulate its biological functions. With their ability to ferry bioactive molecules (eg, proteins and microRNAs) between neighboring and distant cells, EVs are identified as important mediators of inter-cellular communication and are implicated in maintaining normal cell physiology as well as influencing disease progression.¹¹ Inferences on the roles of EVs can thus be determined by analyzing their composition.

Tumor-derived EVs ability to modulate the inflammatory response to affect neurological processes and influence blood brain barrier (BBB) permeability may in part contribute to the pathogenesis of CRCI.^{12,13} Tominaga et al¹⁴ reported that high levels of miR-181c were present in EVs from sera of breast cancer patients who had brain metastases compared to patients without metastasizing cancer cells. It was also reported that miR-181c is related to the brain metastasis of breast cancer patients and their release through EVs promotes the destruction of the BBB through the abnormal localization of actin. Interestingly, chemotherapy could alter the properties of EVs from plasma of breast cancer patient¹⁵ and was found to have thrombogenic effects on endothelial cells,¹⁶ which might be



Creative Commons Non Commercial CC BY-NC: This article is distributed under the terms of the Creative Commons Attribution-NonCommercial 4.0 License (<https://creativecommons.org/licenses/by-nc/4.0/>) which permits non-commercial use, reproduction and distribution of the work without further permission provided the original work is attributed as specified on the SAGE and Open Access pages (<https://us.sagepub.com/en-us/nam/open-access-at-sage>).

indicative for chemotherapy-related thrombogenicity or vascular damage. Indeed, cancer and chemotherapy can alter EVs composition and release, shedding light on the pathogenesis of cancer- and therapy-related adverse events. Other than inflammation and BBB disruption, EVs may potentially interact with the nervous system to affect neurological processes such as neuroplasticity and stress response to adversely impact cognitive abilities in cancer survivors. Improved cognitive and pathophysiological outcomes found in preclinical rodent models injected with stem cell-derived EV following cancer treatment support this idea.^{17,18}

To bridge the knowledge gap between EVs and CRCI, we conducted an exploratory analysis of longitudinal plasma samples of cognitive impaired and non-impaired breast cancer patients who received anthracycline-based chemotherapy, with an overall aim to uncover protein signatures in EVs as potential mediators in regulating the development of CRCI and, potentially serving as biomarkers. Specifically, we characterized the plasma EVs, examined the EV proteomic content and investigated the glycosylation of EV peptides.

Methods

Study design

This was a prospective cohort study conducted at the National Cancer Centre Singapore and KK Women's and Children's Hospital between 2014 and 2017.^{4,19} The study was approved by the Singhealth Institutional Review Board (CIRB 2011/457/B and CIRB 2014/754/B) and written informed consent of patients was obtained.

Eligible patients were at least 21 years of age, diagnosed with early-stage breast cancer (stages I-III), had no prior history of chemotherapy and/or radiation therapy, able to understand either English or Chinese and scheduled to receive anthracycline-based chemotherapy with curative intent. All participants received anthracycline-based therapy (doxorubicin 60 mg/m²/cycle and equivalent) every 3 weeks for 4 cycles. Patients were excluded if they were diagnosed with psychiatric medical conditions.

Patients' self-perceived cognitive abilities were evaluated using the Functional Assessment of Cancer Therapy Cognitive Function (FACT-Cog) (version 3) at 3 time-points: before the start of chemotherapy (T1), at 3 weeks after cycle 2 of chemotherapy (T2), and at 3 weeks after the last cycle of anthracycline chemotherapy (T3). Correspondingly, blood drawing was performed at the 3 time-points and the plasma was obtained by centrifuging at 2000 × *g* for 10 minutes and stored at -80°C.

Sample selection

The patients were categorized into either the cognitive non-impaired (CNI; *n* = 29) or impaired (CI; *n* = 29) group based on a clinically important reduction (10.6-point) in the global FACT-Cog score between the assessed time-points (T3 vs T1

and/or T2 vs T1).^{19,20} Clinical characteristics and demographics were similar between the 2 groups (Table 1). To normalize biological variation, plasma from multiple individuals within each group were combined in equal proportions to obtain a total sample volume of 5 mL plasma for analysis.

Extracellular vesicle isolation

EVs were isolated from plasma by differential ultracentrifugation described by Cheow et al.²¹ In brief, 5 mL pooled plasma of the CNI group at T1, T2, and T3 and the CI group at T1, T2, and T3 was diluted with an equal volume of phosphate-buffered saline (PBS; Gibco, Life Technologies Australia Pty Ltd, Mulgrave, Victoria, Australia) and centrifuged at 2000 × *g* (30 minute), and 12000 × *g* (60 minute) to remove intact cells and cellular debris. Plasma EVs were obtained by ultracentrifugation at 100000 × *g* (18 hour) using a Beckman L100-XP Ultracentrifuge (Beckman Coulter, Brea, CA). The supernatant was ultracentrifuged at 200000 × *g* (18 hour) and the pellet collected was used for glycosylation study. Both the EVs and 200000 × *g* pellets were washed in 1 × PBS and pelleted at 100000 × *g* (18 hour) and 200000 × *g* (18 hour) respectively to remove contaminants. The EVs and 200000 × *g* pellets were stored at -80°C until further analyses.

Nanoparticle tracking analysis

The nanoparticle tracking analysis (NTA) was performed using a NanoSight NS300 instrument, with camera type sCMOS (Malvern Panalytical, Malvern, UK).²² The analysis parameters of the instrument were set as follows: capture time 60 seconds, camera level 4, slider shutter 50, slider gain 100, FPS 32.5, syringe pump speed 100, total volume per sample 1 mL, viscosity 0.906 to 0.910 cP and temperature ~24°C. The size distribution and total particle number of the plasma EVs were calculated based on 5 replicate measurements assessed by NTA.

Sodium dodecyl sulfate-polyacrylamide gel electrophoresis (SDS-PAGE) and Western blot analysis

Protein concentrations were determined by Bradford dye assays. Ten microgram proteins were resolved on a 12% polyacrylamide gel, separated by polyacrylamide gel electrophoresis, and transferred onto a polyvinylidene fluoride (PVDF) membrane (Bio-Rad). Western blot analysis was performed using goat polyclonal antibody anti-Flotillin 1 (Flot-1) (1:500 dilution; ab13493 Abcam, Cambridge, UK) and rabbit monoclonal antibody anti-Tumor Susceptibility 101 (TSG101) (1:500 dilution; ab125011 Abcam, Cambridge, UK) as primary antibodies and anti-goat HRP conjugated IgG, and anti-rabbit HRP conjugated IgG as secondary antibodies at 1:1000 dilutions.

Table 1. Demographics and clinical characteristics of participants.

CHARACTERISTICS	COGNITIVE NON-IMPAIRED (N=29)	COGNITIVE IMPAIRED (N=29)	P-VALUE
Age, mean (SD)	50.1 (10.1)	47.7 (9.5)	.35
Ethnicity, n (%)			
Chinese	24 (82.8)	25 (86.2)	1.00
Malay	3 (10.3)	3 (10.3)	
Indian	1 (3.4)	1 (3.4)	
Others	1 (3.4)	0 (0.0)	
Marital status, n (%)			
Single	8 (27.6)	5 (17.2)	.67
Married	19 (65.5)	23 (79.3)	
Divorced	1 (3.4)	1 (3.4)	
Widowed	1 (3.4)	0 (0.0)	
Education level, n (%)			
Primary school	4 (13.8)	7 (24.1)	.53
Secondary school	12 (41.4)	7 (24.1)	
Pre-university	7 (24.1)	9 (31.0)	
Graduate/postgraduate	6 (20.7)	6 (20.7)	
Occupation, n (%)			
Not working	13 (44.8)	9 (31.0)	.29
Working	16 (55.2)	18 (62.1)	
On medical leave	0 (0.0)	2 (6.9)	
ECOG performance status ^a , n (%)			
0	27 (93.1)	26 (89.7)	1.00
1	2 (6.9)	3 (10.3)	
Menopausal status, n (%)			
Pre-menopausal	15 (51.7)	17 (58.6)	.79
Post-menopausal	14 (48.3)	12 (41.4)	
Breast cancer characteristics, n (%)			
HER2 positive	7 (24.1)	9 (31.0)	.77
Estrogen receptor positive	24 (82.8)	19 (65.5)	.23
Progesterone receptor positive	22 (75.9)	16 (55.2)	.17
Triple-negative	4 (13.8)	5 (17.2)	1.00
Breast cancer stage, n (%)			
Stage I	2 (6.9)	1 (3.4)	.69
Stage II	15 (51.7)	13 (44.8)	
Stage III	12 (41.4)	15 (51.7)	
Chemotherapy regimen			

(Continued)

Table 1. (Continued)

CHARACTERISTICS	COGNITIVE NON-IMPAIRED (N=29)	COGNITIVE IMPAIRED (N=29)	P-VALUE
Anthracycline-based	29 (100)	29 (100)	1.00
FACT-Cog (version 3), n (%)			
Cognitive non-impaired	29 (100.0)	0 (0.0)	<.001
Cognitive impaired at both T2 and T3	0 (0.0)	10 (34.5)	
Cognitive impaired at T2 only	0 (0.0)	6 (20.7)	
Cognitive impaired at T3 only	0 (0.0)	13 (44.8)	

Abbreviations: SD, standard deviation; ECOG, Eastern Cooperative Oncology Group; HER2, human epidermal growth factor receptor 2; FACT-Cog, Functional Assessment of Cancer Therapy Cognitive Function.

T1 before the start of chemotherapy, T2 at 3 weeks after cycle 2 of chemotherapy, T3 at 3 weeks after the last cycle of anthracycline chemotherapy.

^aECOG Grade 0 means that the patient is fully active, able to carry on all pre-disease performance without restriction. ECOG Grade 1 means that the patient is restricted in physically strenuous activity but ambulatory and able to carry out work of a light or sedentary nature, for example, light housework, office work.

Transmission electron microscopy

The enriched EVs were transferred onto a copper grid (Electron Microscopy Services, USA), washed in water and fixed with 2.5% glutaraldehyde (Electron Microscopy Services, USA) for 10 minutes. The samples were then contrasted with 2.5% gadolinium triacetate (Electron Microscopy Services, USA) for 2 minutes and examined using a FEI Tecnai 12 transmission electron microscope operated at 100 kv (FEI, USA).

Proteomic Analysis of Plasma EVs by Mass Spectrometry (MS)

Sample preparation and TMT6 labeling

Each pellet was dissolved in a SDS-ABB buffer (2% SDS, 100 mM ammonium bicarbonate (ABB), pH 8.0). The sample was subsequently centrifuged at $10\,000 \times g$, 4°C for 10 minutes, and the supernatants were collected. The protein in the supernatant was further purified by cold acetone precipitation at -20°C for 4 hours. Protein pellet was re-dissolved in a urea-TEAB buffer (8M urea, 25 mM triethylammonium bicarbonate [TEAB], pH 8.5) and the concentration was determined by BCA assay. Reduction, alkylation, and tryptic digestion of proteins were performed as previously described.²³ Briefly, 100 µg proteins was reduced by DTT and alkylated by IAA. The solution was then diluted to 1M urea using 25 mM TEAB buffer before trypsin digestion at 30°C overnight using sequencing grade trypsin (Promega, Wi, USA). The digestion was stopped by acidifying the solution with 5% acetic acid and tryptic peptides were dried using a vacuum concentrator (Eppendorf AG, Hamburg, Germany). Dried tryptic peptides were subsequently labeled with TMT6 tags from Thermo Scientific (IL, USA), and all the peptide labeling procedures were performed according to the manufacturer's protocol. TMT tags were distributed as follows: 126 CI (T1), 127 CI (T2), 128 CI (T3), 129 CNI (T1), 130 CNI (T2), and 131 CNI (T3).

HPLC fractionation

The labeling reactions were quenched, and 6 labeled peptide samples were mixed and dried. PNGase F (P0705L, New England Biolabs Inc.) was then added as per the manufacturer's instructions and incubated at 37°C for 6 hours for complete deglycosylation. Following PNGase F treatment, the TMT6-labeled peptides were desalted using Sep-Pak C18 cartridges, vacuum dried, and fractionated on a XBridge C18 column (4.6×200 mm, 5 µm, 300 Å) (Waters, MA, USA) at a flow rate of 1.0 mL/minute using HPLC. The mobile phases consisting of buffer A (0.02% NH₄OH in water) and buffer B (0.02% NH₄OH in 80% ACN) were used to establish 60-minute gradient as 97% buffer A for 3 min, 3% to 10% buffer B for 2 minutes, 10% to 35% buffer B for 40 min, 35% to 70% buffer B for 5 minutes and 100% buffer B for 10 minutes at 1 mL/minute flow rate. HPLC chromatograms were recorded at 280 nm and 60 fractions were collected using an automated fraction collector. The collected fractions were pooled according to the concatenate pooling method, concentrated using a vacuum centrifuge, and reconstituted in 0.1% formic acid for LC-MS/MS analysis.²⁴

LC-MS/MS analysis

The LC-MS/MS analysis was performed using Dionex Ultimate 3000 RSLC nanoLC system coupled to a Q-Exactive apparatus (Thermo Fisher, MA). 2 µg of protein in each fraction was injected into an acclaim peptide trap column via the autosampler of the Dionex RSLC nanoLC system. Mobile phase A (0.1% FA in 5% ACN) and mobile phase B (0.1% FA in ACN) were used to establish a 60 minute gradient. The flow rate was maintained at 300 nL/minute. Peptides were analyzed on a Dionex EASY-spray column (PepMap® C18, 3 µm, 100 Å) using an EASY nanospray source at an electrospray potential of 1.5 kV. MS scan (350-1600 m/z range) was acquired at a resolution of 70 000 at m/z 200, with a maximum ion

accumulation time of 100 ms. Dynamic exclusion was set to 30 seconds. Resolution for MS/MS spectra was set to 35 000 at m/z 200. The AGC setting was 1E6 for the full MS scan and 2E5 for the MS2 scan. The 10 most intense ions above a 1000 count threshold were selected for HCD fragmentation, with a maximum ion accumulation time of 120 ms. An isolation width of 2 Da was used for the MS2 scan. Single and unassigned charged ions were excluded from MS/MS. For HCD, the normalized collision energy was set to 28. The underfill ratio was defined as 0.1%.²⁴

Database search and data analysis

Acquired data was further processed using Proteome Discoverer v2.2 (PD2.2, Thermo Scientific, San Jose, USA). The raw files were directly imported into the PD with deisotope and deconvolution in MS/MS spectra. The processed MS/MS spectra were queried against a Uniprot human database (downloaded on 6th February 2017 with 61972042 sequences and 1486340556 residues) using both SequestHT and Mascot search engines. The parameters set were enzyme: trypsin; maximum miss cleavage: 2; precursor mass tolerance: 10 ppm; fragment mass tolerance: 0.02 Da; fixed modification: carbamidomethylation at Cys and TMT6 at peptide N-terminal and Lys; dynamic modification: Oxidation at Met, deamidation at Asp and Gln; The peptide spectral matches (PSMs) were further processed by “percolator” algorithm where target FDR (strict) was set as 0.01, target FDR (relaxed) was set as 0.05. The relative protein quantitation based on the TMT reporter ions was performed using the default method for TMT 6plex labeling in the consensus workflow of PD2.2. The result data was exported to a text file that was then imported to Microsoft Excel for further analysis. Only proteins that showed a False Discovery Rate (FDR) of q -value < 0.01 were considered for further analysis. The dataset was screened against the Harmonizome database²⁵ which integrated the curated Gene-Disease Association datasets associated with cognitive disorders retrieved from the Comparative Toxicogenomics Database²⁶ (http://amp.pharm.mssm.edu/Harmonizome/gene_set/Cognition+Disorders/CTD+Gene-Disease+Associations). The mass spectrometry proteomics data have been deposited to the ProteomeXchange Consortium (<http://proteomecentral.proteomexchange.org>) via the PRIDE partner repository²⁷ with the dataset identifier (PXD021395).

Statistical analyses

For demographics and clinical characteristics, Fisher's exact test was performed to test for differences between categorical variables. Continuous variables were analyzed with independent sample t -test. Protein expression at each time-point was normalized against the expression at T1. Student's t -test was used to identify statistically significant differences between 2

time-points (T2 vs T1 and T3 vs T1) for the 2 groups (CNI and CI). Prism Software (prism7, GraphPad Inc., La Jolla, CA) was used for the statistical test. Data were presented as sample means \pm SD. Statistical significance was defined as $P < .05$.

Results

Extracellular vesicles characterization

EVs derived from human plasma were enriched and characterized using NTA, transmission electron microscopy, and Western blot (Figure 1). Figure 1a and b showed the mean particle size and the yield of plasma EVs of CNI and CI groups at T1, T2, and T3. There were no significant time-point differences observed in the EV size and particle number in the 2 groups. Western blot results (Figure 1c) showed the presence of EV markers, flotillin 1 (Flot-1), and tumor susceptibility gene 101 (TSG101) proteins. Transmission electron microscopy confirmed the spherical shaped morphology of the EVs (Figure 1d).

Mass spectrometric analysis of plasma EVs from CNI and CI patients

TMT quantitative proteomic analysis of plasma EVs from CNI and CI patients at 3 time-points (T1, T2, and T3) identified a total of 517 differentially expressed proteins (Supplemental Table 1), with a set false discovery rate (FDR) of $> 1\%$ for proteins and at least 2 peptides above the 95% confidence area. Known EV markers, including CD9 (accession number G8JLH6), TSPAN14 (accession number Q8NG11), and CD5L (accession number O43866) were detected in the EV samples of CNI and CI patients by LC-MS/MS.

Mass spectrometric analyses of plasma EVs from CNI patients showed a downregulation of galactosylceramidase (accession number A0A024R6E8, 24.2% reduction, $P < .01$), and upregulation of p2X purinoceptor (accession number B2R876, 1.1 fold increase, $P < .01$) and cofilin-1 (accession number E9PK25, 1.3 fold increase, $P < .05$) at T3 when compared to the T1 baseline (Figure 2). In contrast, plasma EVs from CI patients showed significant decrease in the expression of p2X purinoceptor (21.6% reduction, $P < .01$), cofilin-1 (24.9% reduction, $P < .05$), nexilin (accession number Q0ZGT2, 38.3% reduction, $P < .01$), and a disintegrin and metalloprotease 10 (ADAM10; accession number A0A024R5U5, 25.2% reduction, $P < .01$) at T3 when compared to the T1 baseline (Figure 2).

Interestingly, the transcription factor IIIB 90 kDa subunit (accession number Q92994) was found to be upregulated in both the plasma EVs of CNI and CI patients at T3 when compared to the T1 baseline (Figure 2f). A 1.6-fold ($P < .01$) increase in the expression of the transcription factor IIIB 90 kDa subunit was detected in the plasma EVs of CNI patients. Additionally, a 2.1-fold ($P < .001$) increase in the expression of the transcription factor IIIB 90 kDa subunit was found in the plasma EVs of CI patients.

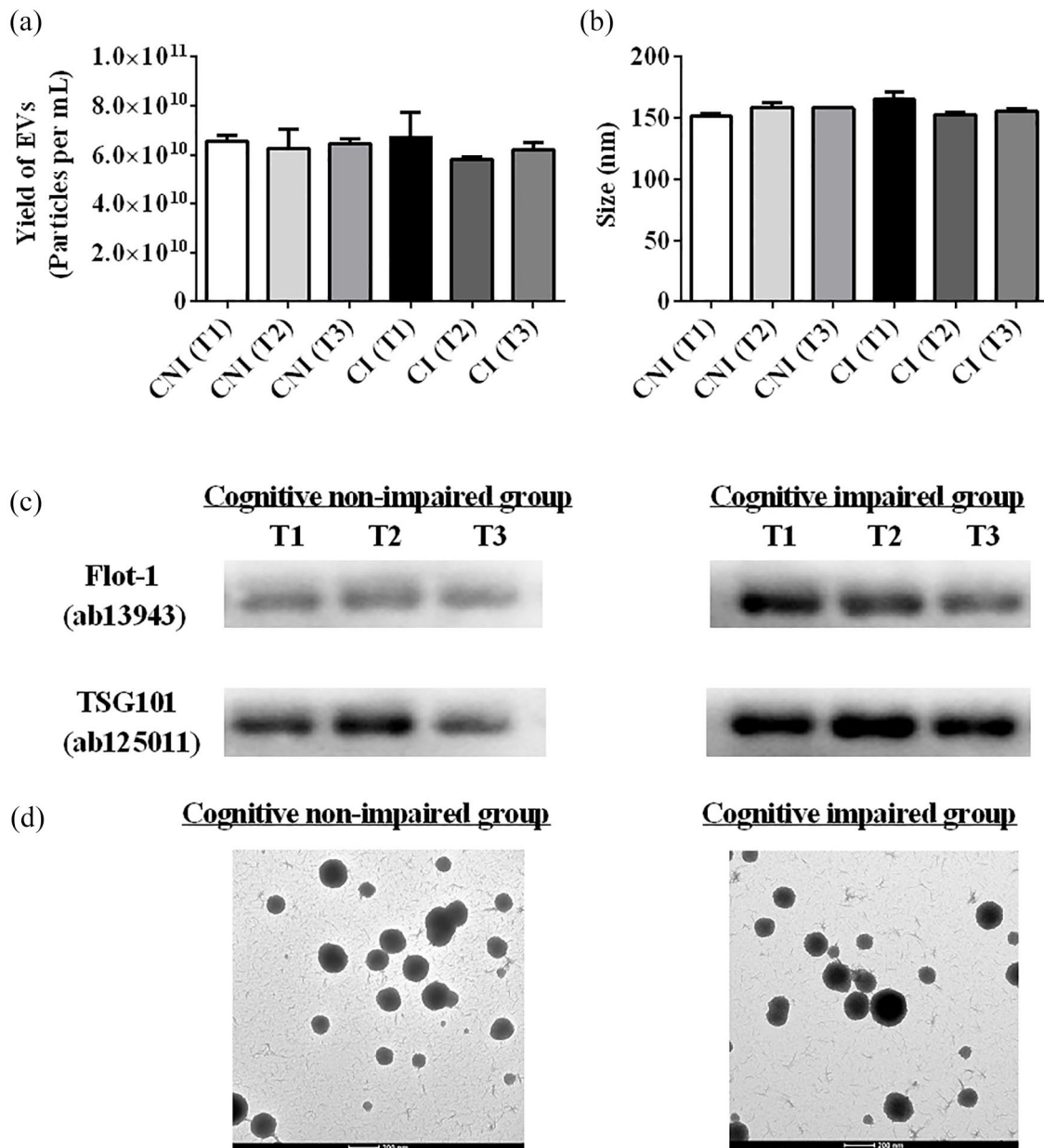


Figure 1. Characterization of extracellular vesicles from Cognitive Non-impaired (CNI) and Impaired (CI) Patients at T1, T2, and T3. The nanoparticle tracking analysis was employed to determine: (a) the concentration (particles per mL), (b) size (nm) of extracellular vesicles based on 5 replicate measurements of the enriched extracellular vesicles from pooled plasma from CNI (n=29) and CI (n=29) patients at T1, T2, and T3, (c) Western blot identified the presence of extracellular vesicle markers flotillin 1 (Flot-1) and tumor susceptibility gene 101 (TSG101) proteins from the enriched extracellular vesicles of pooled plasma, and (d) a representative electron micrograph showing the spherical morphology of extracellular vesicles, Scale bar 200nm. Results are presented as means \pm SD.

Dynamin-1 expression in EVs of CNI and CI patients was decreased at T3

Dynamin-1 (accession number A0A0D9SFE4) expression in both the plasma EVs of CNI and CI patients was observed to be significantly reduced at T3 when compared to the T1 baseline (Figure 3). Dynamin-1 was found to have a 17.7% decrease in expression in CNI (86.27 ± 0.59 arbitrary units vs 104.87 ± 2.70 arbitrary units for T3 and T1, respectively, $P < .01$) compared to a 43.6% decrease in expression in the CI patients (74.23 ± 0.55 arbitrary units vs 131.60 ± 7.71 arbitrary

units for T3 and T1, respectively, $P < .01$). The downregulation of dynamin-1 in plasma EVs was approximately 1.2 times more in the CI than in the CNI patients at T3.

Tight junction protein Eexpression in EVs was greatly reduced in CI patients at T3

Tight junction proteins, including the tight junction protein zonula occludens-2 (ZO-2 accession number A0A1B0GTW1), junctional adhesion molecule C (JAM-C; accession number Q9BX67), and claudin (accession number D3DX19) were

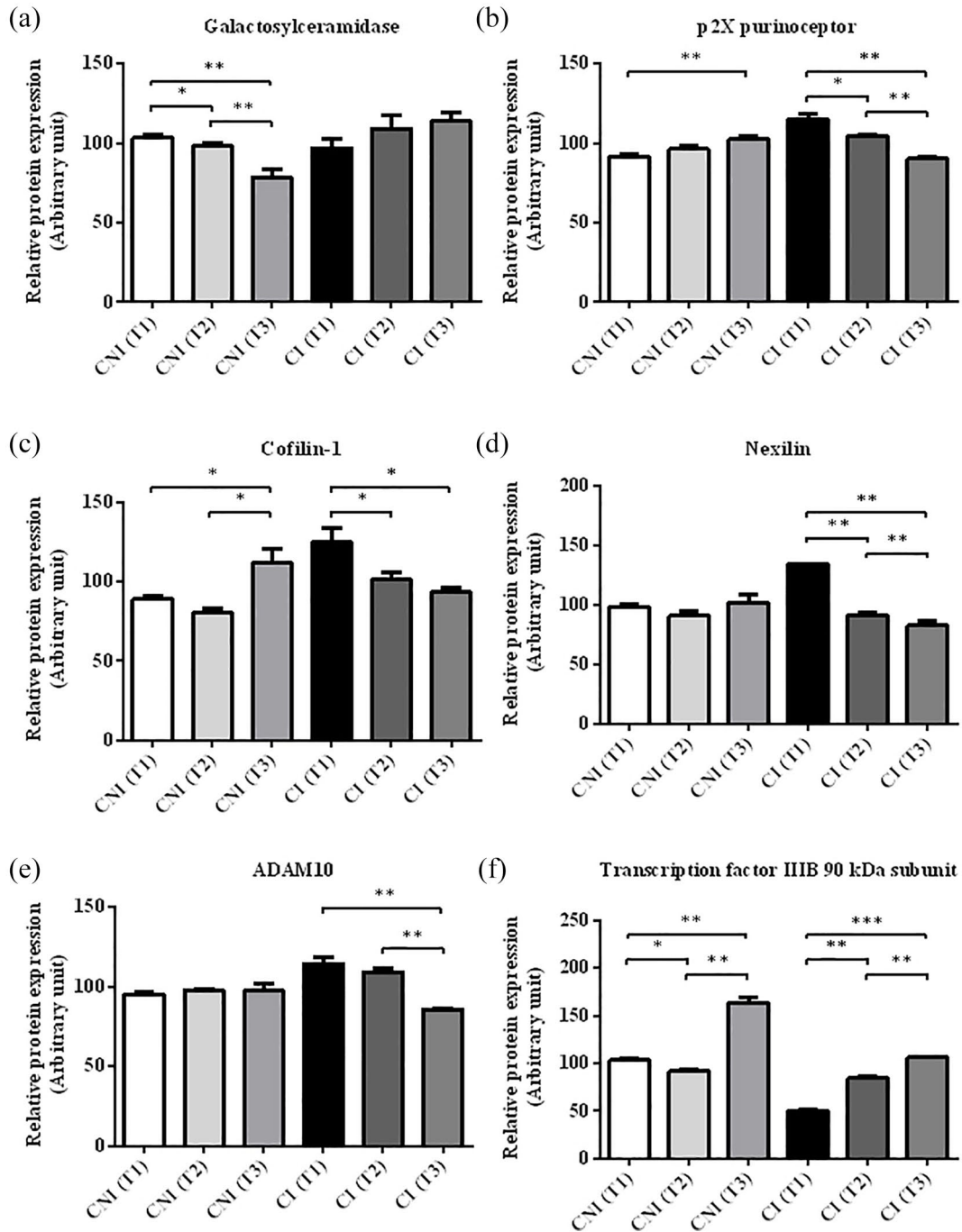


Figure 2. Expression of EV proteins from Cognitive Non-impaired (CNI) and Impaired (CI) patients at T1, T2, and T3. The relative protein expression (arbitrary units) of: (a) galactosylceramidase, (b) p2X purinoceptor, (c) cofilin-1, (d) nexilin, (e) ADAM10, and (f) transcription factor IIIB 90kDa subunit from plasma EVs of CNI and CI patients compared across time-points T1, T2, and T3. Results are presented as means \pm SD ($n=3$), and protein expression was normalized against expression at T1. Differences of $*P < .05$, $**P < .01$ and $***P < .001$ were considered statistically significant.

detected in the plasma EVs of CNI and CI patients by mass spectrometry (Figure 4). The tight junction protein ZO-2 (Figure 4a) in the plasma EVs of CI patients was found to have a 41.7% decrease in expression at T3 (78.63 ± 5.40 arbitrary units, $P < .05$) when compared to the T1 baseline (134.80 ± 5.87 arbitrary units). The JAM-C (Figure 4b) and claudin (Figure 4c) in the plasma EVs of CI patients, when compared between T3 and T1 baseline, were also found to have a 27.2% reduction (90.97 ± 11.38 arbitrary units at T3 vs

124.93 ± 6.88 arbitrary units at T1, $P < .01$), and a 53.2% reduction (70.83 ± 1.04 arbitrary units at T3 vs 151.43 ± 1.63 arbitrary units at T1, $P < .001$) in their expression respectively. While tight junction protein ZO-2 (Figure 4a) and JAM-C (Figure 4b) was not altered in the plasma EVs of CNI patients when compared between T3 and T1 baseline, a 4.5% decrease was observed in claudin expression (91.77 ± 2.45 arbitrary units vs 96.13 ± 2.14 arbitrary units for T3 and T1, respectively, $P < .05$) (Figure 4c).

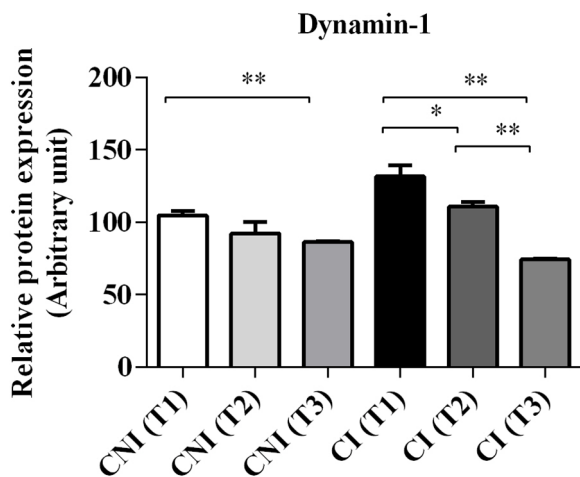


Figure 3. Dynamin-1 expression in Cognitive Non-impaired (CNI) and Impaired (CI) patients at T1, T2 and T3. The relative protein expression (arbitrary units) of dynamin-1 in plasma EVs of CNI and CI patients compared across time-points T1, T2, and T3. Results are presented as means \pm SD ($n=3$), and protein expression was normalized against expression at T1. Differences of $*P < .05$ and $**P < .01$ were considered statistically significant.

N-linked glycosylation of peptides of EV proteins from CNI and CI patients

The mass spectrometry identification of N-linked glycosylation sites generally depends on the detection of asparagine deamidation in the consensus sequence N-X-S/T/C (with X not proline) in peptides after PNGase F treatment. The mass spectrometry detected glycosylation of several plasma EVs proteins by PNGase F (Supplemental Table S2). However, no glycosylation was observed in the peptides of galactosylceramidase, nexilin, p2X purinoceptor, cofilin-1, ADAM 10, transcription factor IIIIB 90 kDa subunit, dynamin-1 and tight junction proteins. Interestingly, the mass spectrometry detected glycosylation at the [R].LVGGDNLCSGR.[L] and [K].NTCNHDEDTWVECEDPFDLR.[L] peptide of CD5L, a marker of EVs²⁸ in both the plasma EVs of CNI and CI patients (Supplemental Table S2).

Discussion

In this study, the EVs enriched from plasma of breast cancer patients showed spherical morphology, presence of EV markers, and no difference in EV numbers across the 3 time-points in the CNI and CI groups. Proteins including p2X purinoceptor, cofilin-1, ADAM 10, galactosylceramidase, nexilin, transcription factor IIIIB 90 kDa subunit, dynamin-1, and tight junction proteins were differentially expressed between the 2 groups. These proteins were not identified to be glycosylated by PNGase F (Supplemental Table S2) and were discovered to be associated with cognitive disorder based on Gene-Disease Association dataset curated from the Comparative Toxicogenomics Database²⁶ in the Harmonizome web portal.²⁵ Interestingly, CD5L protein which was previously reported as a suitable marker for MS-based proteomic analysis of plasma-derived vesicles,²⁸ was detected to

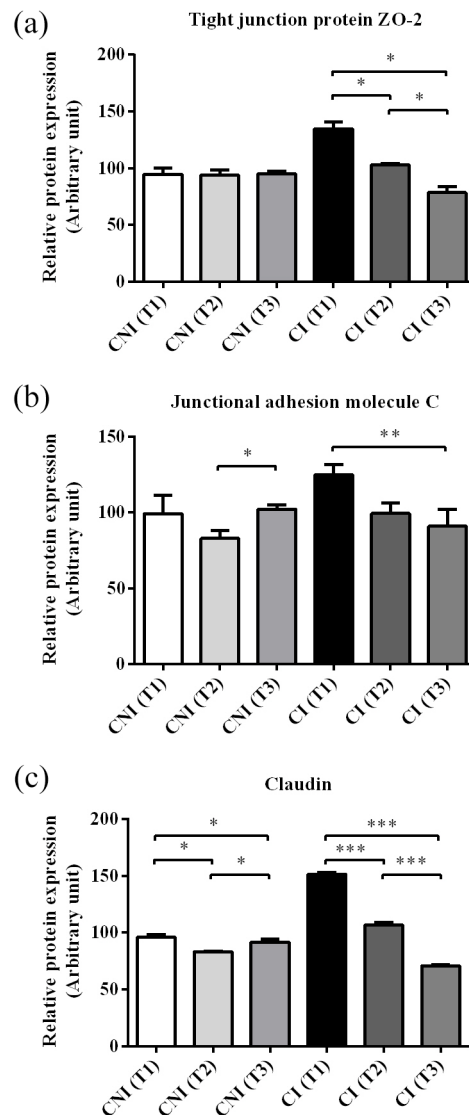


Figure 4. Tight junction protein expression in Cognitive Non-impaired (CNI) and Impaired (CI) patients at T1, T2, and T3. The relative protein expression (arbitrary units) of: (a) tight junction protein ZO-2, (b) junction adhesion molecule C, and (c) Claudin in plasma EVs of CNI and CI patients compared across time-points T1, T2, and T3. Results are presented as means \pm SD ($n=3$), and protein expression was normalized against expression at T1. Differences of $*P < .05$, $**P < .01$ and $***P < .001$ were considered statistically significant.

have specific deamidation at the [R].LVGGDNLCSGR.[L] and at the [K].NTCNHDEDTWVECEDPFDLR.[L] peptide of CD5L. The decreased CD5L glycosylation at [K].NTCNHDEDTWVECEDPFDLR.[L] in the CNI participants but not the CI participant at T3 compared to the T1 baseline, indicates a difference in the CD5L glycosylation patterns. As there have been reports of differential CD5L glycosylation leading to distinct functional activities of CD5L biology,^{29,30} our findings suggest a different functional aspect of CD5L between the CI and CNI groups, which could potentially influence EVs delivery, their interaction and uptake by recipient cell.³¹ Overall, our results suggest that EVs contain proteins that may participate in modulating the cellular mechanisms to affect nervous system

activity and the BBB. Additionally, these results suggest the potential for these EV proteins to interact with the central nervous system (CNS) to affect cognitive abilities in breast cancer patients receiving anthracycline-based chemotherapy.

In our findings, the expressions of p2X purinoceptor,³² cofilin-1,³³ and ADAM 10³⁴ were downregulated in the CI group after anthracycline chemotherapy, proteins that possess essential roles in the molecular mechanisms underlying synaptic plasticity, learning and memory.³⁵⁻³⁸ Within the plastic regions of the brain (like hippocamps), cofilin play an essential role in remodeling actin filaments and spinogenesis to preserve the long-term potentiation and thereby synaptic plasticity.³⁹⁻⁴¹ Studies have highlighted that the dysregulation of p2X purinoceptor,⁴² cofilin-1,⁴³ and ADAM 10^{44,45} are implicated in CNS pathology such as Alzheimer's disease, suggesting that the pathophysiology of CRCI may not be substantially different from other CNS disorders. While not a focus of the current study, these proteomic signatures may also provide potential insight into chemotherapy-induced peripheral neuropathies, another outcome that adversely impacts the quality of life of breast cancer survivors.^{46,47}

Interestingly, expression of galactosylceramidase was unchanged in plasma EVs of CI group but was downregulated in the plasma EVs of CNI group after anthracycline chemotherapy. On the other hand, nexilin expression was downregulated in the CI group but remained unchanged among CNI patients. Both proteins play important roles in myelin regulation. Galactosylceramidase is an enzyme important in the production of normal myelin^{48,49} and nexilin has been found to participate in oligodendrocyte progenitor cell (OPC) recruitment and remyelination.⁵⁰ These results suggest that a different regulatory mechanism may be activated for the maintenance of myelin integrity and function in the CNI and CI groups, contributing to the disparity in cognitive abilities between the 2 groups of patients. Furthermore, as OPC is important for the regeneration of myelin and oligodendrocytes post-injury or disease,⁵¹ decreased OPC recruitment might be implicated with reduced expression of nexilin among CI patients, potentially impairing cognitive recovery.

Transcription factor IIIIB was observed to be upregulated in both CNI and CI groups after anthracycline chemotherapy. It was recently reported that mutation of the transcription factor IIIIB caused neurodevelopmental anomalies.⁵² The literature describes that the activity of transcription factor IIIIB is regulated by mitogen-activated protein kinase and extracellular signal-regulated kinase pathways, and functions to promote cell growth and proliferation,⁵³ which could be essential for neurodevelopment.⁵⁴ However, whether transcription factor IIIIB activity could affect the expression of protein-coding genes in the CNS⁵⁵ and is important for normal cerebellar and cognitive development⁵² remains to be elucidated.

The present study observed a greater reduction of dynamin-1 expression in the plasma EVs of CI than in the CNI patients at

T3 compared to the T1 baseline. Previous studies in mouse model^{56,57} demonstrated that a decreased expression in dynamin-1 could cause defects in the biogenesis and endocytic recycling of synaptic vesicles and this could impact neuronal ability to regulate synaptic transmission. In a clinical assessment of post-mortem brains, it was discovered that reduced levels of dynamin-1 were correlated with a higher rate of cognitive decline and this was observed in cases of patients with dementia.⁵⁸ Interestingly, dynamin-1 was involved in memory formation,⁵⁹ a subset of the cognitive domains defined by ICCTF.^{60,61} The downregulation of dynamin-1 expression detected in the plasma EVs of the CNI and CI patients may suggest a negative impact of cancer and/or chemotherapy on memory and cognition functioning. Despite reduced dynamin-1 in both CNI and CI groups, we found a greater impact in the CI group (1.2 times reduction) compared to CNI at T3 time point. This observation emphasizes an ongoing disruption in vesicular trafficking, in general, and warrants further investigation using transgenic knock-in or knock-out mouse models.⁶²

Additionally, tight junction protein expression (ie, tight junction protein ZO-2, JAM-C, and claudin) was found to be greatly reduced in plasma EVs of CI but not CNI patients after anthracycline chemotherapy. Significant advances in BBB research have described the critical role of tight junction and adherens junction proteins, in creating a dynamic barrier system, and regulating the paracellular transport of solutes and ions between the blood and brain.⁶³ The disruption of BBB is an extensively investigated hypothesis behind neurotoxin-induced and disease-related cognitive impairment. The tight junction proteins are essential to maintain the overall integrity and permeability of the blood-brain and blood-spinal cord barrier^{64,65} which has been shown to be compromised by cancer therapies. For example, exposure to clinically relevant cranial radiation therapy for brain cancers disrupts BBB which was associated with elevated oxidative stress and inflammation.⁶⁵⁻⁶⁷ Previously, studies reporting the exposure of neurotoxicants malathion and lead acetate⁶⁸ or high glucose (25 mmol/L D-glucose)⁶⁹ could lead to an induced reduction of tight junction protein ZO, claudin, and occludin expression in brain microvascular endothelial cells which results in increased permeability of the BBB. In contrast, the use of Scutellarin or Scutellarin-treated EVs was demonstrated to exert protective effect on brain microvascular endothelial cells by reducing homocysteine-mediated damage to tight junction proteins.⁷⁰ Moreover, the inhibition of glycogen synthase kinase 3 β activity was shown to exhibit improved cognitive function in aged mice by upregulating claudin and restores BBB integrity.⁷¹ It is plausible that an association exists between tight junction disruption and the breakdown of BBB, and the decreased tight junction protein expression in the plasma EVs of CI patients may be indicative of tight junction disruption via EV-related biological activities, resulting in vascular cognitive impairment in the CI patients. In the end, it is difficult to conclude precisely

how BBB disruption impacts neurocognitive functionality without overt and/or persistent changes in cerebral blood flow. However, potential disruption to cerebrovascular integrity brought on by chemotherapy may portend an elevated risk of CNS microbleeds, ischemia and stroke.^{72,73} As tight junction proteins ZO-2 and JAM-C were not altered in the plasma EVs of CNI patients when compared between T3 and T1 baseline, our findings suggest that these proteins may have been tightly regulated for maintaining the stability and function of the BBB unlike CI patients.⁷⁴

While there is substantial interest in understanding cognitive decline after cancer treatment, progress in the field is hindered by the inability to discern the exact cause of cognitive decline complicated by many factors including other cancer treatment modalities (eg, hormone therapy, radiotherapy), aging, and psychosocial factors (eg, fatigue, anxiety, and depression). Moreover, few studies have examined the longitudinal association of cognitive deficits and cancer treatment, which analyzed cognitive function at different stages of cancer treatment and survivorship. We postulate that patients' differential responses to therapy have led to the differential protein expression observed between the 2 groups. Chemotherapeutic agents, such as vincristine, oxaliplatin, and cisplatin, have been shown to influence genes associated with the immune system, causing different degree of toxicities observed in patients receiving the same treatments.⁷⁵ Similarly, another study has demonstrated that high levels of major histocompatibility complex processing, presentation proteins, and lipid metabolism proteins were associated with poor therapeutic responses in breast cancer patients.⁷⁶ It is likely that chemotherapeutic agents can induce changes and impact on the expressions of genes and proteins among different patients. Our findings provide insights on the protein expression profiles of EVs from plasma of self-perceived cognitive impairment of breast cancer patients before, during and after treatment of anthracycline-based chemotherapy thus potentially provide biomarker discovery avenue predictive of CRCI long-term after cessation of cancer therapy. In conclusion, differential expression of several EV proteins may potentially affect the biological processes of the CNS and BBB to impact cognitive functioning in breast cancer patients. Consistent with findings reported by Brown et al, proteins such as dynamin-1 and cell-cell junction proteins within the key metabolic and signaling pathways were downregulated and were associated with cognitive dysfunction, as a result of chemotherapy treatment.⁷⁷ Furthermore, chemotherapy-induced changes in the junctional and cytoskeletal apparatus of endothelial cells were demonstrated, and these alterations may affect BBB integrity leading to brain dysfunction.⁷⁸ This study substantiates a link between EVs and cognitive functioning and represents a starting point for further investigation. Future evaluation of EVs isolated from a larger cohort with a healthy control, and studying their interactions with CNS and BBB cells, will strengthen the link

between EVs, CRCI, cancer, and cancer treatments. Importantly, the characterization of EVs from plasma of patients with breast cancer may unravel key mechanisms underlying CRCI and identify potential biomarkers of CRCI to guide the development of precision assessment and effective interventions for patients at risk for CRCI.

Acknowledgements

The authors acknowledge all the researchers and technicians who supported this study and thank all the volunteers that participated in this study.

Author Contributions

Conceived, designed, and interpreted the data sets (Y.Q.K. and A.C.). Performed experiments, statistical analysis of the data sets, wrote and prepared figures for the manuscript (Y.Q.K. and D.Q.N.). Designed, performed, and interpreted data of mass spectrometry experiments (Y.Q.K., C.C.N., M.W., S.K.S. and A.C.). Performed transmission electron microscopy (A.B.). Provided ideas, discussions and supervised the study (S.K.S., H.K.H., M.A., C.L.L. and A.C.). Revised and approved the final version of manuscript (Y.Q.K., D.Q.N., C.C., A.B., M.W., S.K.S., H.K.H., M.A., C.L.L. and A.C.).

ORCID iD

Ding Quan Ng  <https://orcid.org/0000-0002-0754-7901>

Supplemental Material

Supplemental material for this article is available online.

REFERENCES

1. Chan RJ, McCarthy AL, Devenish J, Sullivan KA, Chan A. Systematic review of pharmacologic and non-pharmacologic interventions to manage cognitive alterations after chemotherapy for breast cancer. *Eur J Cancer*. 2015;51:437-450.
2. Hardy SJ, Krull KR, Wefel JS, Janelins M. Cognitive changes in cancer survivors. *Am Soc Clin Oncol Educ Book*. 2018;38:795-806.
3. Cheung YT, Chui WK, Chan A. Neuro-cognitive impairment in breast cancer patients: pharmacological considerations. *Crit Rev Oncol Hematol*. 2012;83:99-111.
4. Ng T, Dorajoo SR, Cheung YT, et al. Distinct and heterogeneous trajectories of self-perceived cognitive impairment among Asian breast cancer survivors. *Psychooncology*. 2018;27:1185-1192.
5. Cheung YT, Shwe M, Tan YP, Fan G, Ng R, Chan A. Cognitive changes in multiethnic Asian breast cancer patients: a focus group study. *Ann Oncol*. 2012;23:2547-2552.
6. Kobayashi LC, Cohen HJ, Zhai W, et al. Cognitive function prior to systemic therapy and subsequent well-being in older breast cancer survivors: longitudinal findings from the Thinking and Living with Cancer Study. *Psychooncology*. 2020;29:1051-1059.
7. Barlow-Krelina E, Chen Y, Yasui Y, et al. Consistent physical activity and future neurocognitive problems in adult survivors of childhood cancers: a report from the childhood cancer survivor study. *J Clin Oncol*. 2020;38:2041-2052.
8. Bray VJ, Dhillon HM, Bell ML, et al. Evaluation of a web-based cognitive rehabilitation program in cancer survivors reporting cognitive symptoms after chemotherapy. *J Clin Oncol*. 2017;35:217-225.
9. Lowry MC, Gallagher WM, O'Driscoll L. The role of exosomes in breast cancer. *Clin Chem*. 2015;61:1457-1465.
10. Sadvovska L, Eglitis J, Line A. Extracellular vesicles as biomarkers and therapeutic targets in breast cancer. *Anticancer Res*. 2015;35:6379-6390.
11. Thompson AG, Gray E, Heman-Ackah SM, et al. Extracellular vesicles in neurodegenerative disease - pathogenesis to biomarkers. *Nat Rev Neurol*. 2016;12:346-357.

12. Olson B, Marks DL. Pretreatment cancer-related cognitive impairment-mechanisms and outlook. *Cancers (Basel)*. 2019;11:687.
13. Koh YQ, Tan CJ, Toh YL, et al. Role of exosomes in cancer-related cognitive impairment. *Int J Mol Sci*. 2020;21:2755.
14. Tominaga N, Kosaka N, Ono M, et al. Brain metastatic cancer cells release microRNA-181c-containing extracellular vesicles capable of destructing blood-brain barrier. *Nat Commun*. 2015;6:6716.
15. Aharon A, Sabbah A, Ben-Shaul S, et al. Chemotherapy administration to breast cancer patients affects extracellular vesicles thrombogenicity and function. *Oncotarget*. 2017;8:63265-63280.
16. Aharon A, Sabbah AR, Issman L, et al. Effects of low- and high-dose chemotherapy agents on thrombogenic properties of extracellular vesicles derived from breast cancer cell lines. *Thromb Haemost*. 2018;118:480-489.
17. Baulch JE, Acharya MM, Allen BD, et al. Cranial grafting of stem cell-derived microvesicles improves cognition and reduces neuropathology in the irradiated brain. *Proc Natl Acad Sci U S A*. 2016;113:4836-4841.
18. Smith SM, Giedzinski E, Angulo MC, et al. Functional equivalence of stem cell and stem cell-derived extracellular vesicle transplantation to repair the irradiated brain. *Stem Cells Transl Med*. 2020;9:93-105.
19. Toh YL, Wang C, Ho HK, Chan A. Distinct cytokine profiles across trajectories of self-perceived cognitive impairment among early-stage breast cancer survivors. *J Neuroimmunol*. 2020;342:577196.
20. Toh YL, Shariq Mujtaba J, Bansal S, et al. Prechemotherapy levels of plasma dehydroepiandrosterone and its sulfated form as predictors of cancer-related cognitive impairment in patients with breast cancer receiving chemotherapy. *Pharmacotherapy*. 2019;39:553-563.
21. Cheow ES, Cheng WC, Lee CN, de Kleijn D, Sorokin V, Sze SK. Plasma-derived extracellular vesicles contain predictive biomarkers and potential therapeutic targets for Myocardial Ischemic (MI) injury. *Mol Cell Proteomics*. 2016;15:2628-2640.
22. Gallart-Palau X, Serra A, Hase Y, et al. Brain-derived and circulating vesicle profiles indicate neurovascular unit dysfunction in early Alzheimer's disease. *Brain Pathol*. 2019;29:593-605.
23. Paramasivan S, Adav SS, Ngan SC, et al. Serum albumin cysteine trioxidation is a potential oxidative stress biomarker of type 2 diabetes mellitus. *Sci Rep*. 2020;10:6475.
24. Adav SS, Park JE, Sze SK. Quantitative profiling brain proteomes revealed mitochondrial dysfunction in Alzheimer's disease. *Mol Brain*. 2019;12:8.
25. Rouillard AD, Gundersen GW, Fernandez NF, et al. The harmonizome: a collection of processed datasets gathered to serve and mine knowledge about genes and proteins. *Database (Oxford)*. 2016;2016:baw100.
26. Davis AP, Grondin CJ, Johnson RJ, et al. The comparative toxicogenomics database: update 2017. *Nucleic Acids Res*. 2017;45:D972-D978.
27. Vizcaino JA, Deutsch EW, Wang R, et al. ProteomeXchange provides globally coordinated proteomics data submission and dissemination. *Nat Biotechnol*. 2014;32:223-226.
28. de Menezes-Neto A, Saez MJ, Lozano-Ramos I, et al. Size-exclusion chromatography as a stand-alone methodology identifies novel markers in mass spectrometry analyses of plasma-derived vesicles from healthy individuals. *J Extracell Vesicles*. 2015;4:27378.
29. Sanjurjo L, Aran G, Roher N, Valledor AF, Sarrias MR. AIM/CD5L: a key protein in the control of immune homeostasis and inflammatory disease. *J Leukoc Biol*. 2015;98:173-184.
30. Kim WK, Hwang HR, Kim DH, et al. Glycoproteomic analysis of plasma from patients with atopic dermatitis: CD5L and ApoE as potential biomarkers. *Exp Mol Med*. 2008;40:677-685.
31. Rosa-Fernandes L, Rocha VB, Carregari VC, Urbani A, Palmisano G. A perspective on extracellular vesicles proteomics. *Front Chem*. 2017;5:102.
32. Pankratov Y, Lalo U, Krishnal OA, Verkhatsky A. P2X receptors and synaptic plasticity. *Neuroscience*. 2009;158:137-148.
33. Wolf M, Zimmermann AM, Gorlich A, et al. ADF/Cofilin controls synaptic actin dynamics and regulates synaptic vesicle mobilization and exocytosis. *Cereb Cortex*. 2015;25:2863-2875.
34. Musardo S, Marcello E, Gardoni F, Di Luca M. ADAM10 in synaptic physiology and pathology. *Neurodegener Dis*. 2014;13:72-74.
35. Gorlich A, Wolf M, Zimmermann AM, et al. N-cofilin can compensate for the loss of ADF in excitatory synapses. *PLoS One*. 2011;6:e26789.
36. Schuck F, Wolf D, Fellgiebel A, Endres K. Increase of alpha-secretase ADAM10 in platelets along cognitively healthy aging. *J Alzheimers Dis*. 2016;50:817-826.
37. Endres K, Deller T. Regulation of alpha-secretase ADAM10 In vitro and in vivo: genetic, epigenetic, and protein-based mechanisms. *Front Mol Neurosci*. 2017;10:56.
38. Lalo U, Palygin O, Verkhatsky A, Grant SG, Pankratov Y. ATP from synaptic terminals and astrocytes regulates NMDA receptors and synaptic plasticity through PSD-95 multi-protein complex. *Sci Rep*. 2016;6:33609.
39. Krucker T, Siggins GR, Halpain S. Dynamic actin filaments are required for stable long-term potentiation (LTP) in area CA1 of the hippocampus. *Proc Natl Acad Sci U S A*. 2000;97:6856-6861.
40. Chen LY, Rex CS, Casale MS, Gall CM, Lynch G. Changes in synaptic morphology accompany actin signaling during LTP. *J Neurosci*. 2007;27:5363-5372.
41. Kramar EA, Chen LY, Brandon NJ, et al. Cytoskeletal changes underlie estrogen's acute effects on synaptic transmission and plasticity. *J Neurosci*. 2009;29:12982-12993.
42. Zarrinmayeh H, Territo PR. Purinergic receptors of the central nervous system: biology, PET ligands, and their applications. *Mol Imaging*. 2020;19:1536012120927609.
43. Barone E, Mosser S, Fraering PC. Inactivation of brain Cofilin-1 by age, Alzheimer's disease and gamma-secretase. *Biochim Biophys Acta*. 2014;1842:2500-2509.
44. Marcello E, Borroni B, Pelucchi S, Gardoni F, Di Luca M. ADAM10 as a therapeutic target for brain diseases: from developmental disorders to Alzheimer's disease. *Expert Opin Ther Targets*. 2017;21:1017-1026.
45. Brummer T, Muller SA, Pan-Montojo F, et al. NrCAM is a marker for substrate-selective activation of ADAM10 in Alzheimer's disease. *EMBO Mol Med*. 2019;11:e9695.
46. Hausheer FH, Schilsky RL, Bain S, Berghorn EJ, Lieberman F. Diagnosis, management, and evaluation of chemotherapy-induced peripheral neuropathy. *Semin Oncol*. 2006;33:15-49.
47. Bandos H, Melnikow J, Rivera DR, et al. Long-term peripheral neuropathy in breast cancer patients treated with adjuvant chemotherapy: NRG Oncology/NSABP B-30. *J Natl Cancer Inst*. 2018;110:djx162.
48. De Gasperi R, Friedrich VL, Perez GM, et al. Transgenic rescue of Krabbe disease in the twitcher mouse. *Gene Ther*. 2004;11:1188-1194.
49. Rafi MA, Zhi Rao H, Passini MA, et al. AAV-mediated expression of galactocerebrosidase in brain results in attenuated symptoms and extended life span in murine models of globoid cell leukodystrophy. *Mol Ther*. 2005;11:734-744.
50. Li Q, Zhao H, Pan P, et al. Nexilin regulates oligodendrocyte progenitor cell migration and remyelination and is negatively regulated by protease-activated receptor 1/Ras-proximate-1 signaling following subarachnoid hemorrhage. *Front Neurol*. 2018;9:282.
51. Hughes EG, Kang SH, Fukaya M, Bergles DE. Oligodendrocyte progenitors balance growth with self-repulsion to achieve homeostasis in the adult brain. *Nat Neurosci*. 2013;16:668-676.
52. Borck G, Hog F, Dentici ML, et al. BRF1 mutations alter RNA polymerase III-dependent transcription and cause neurodevelopmental anomalies. *Genome Res*. 2015;25:155-166.
53. Goodfellow SJ, White RJ. Regulation of RNA polymerase III transcription during mammalian cell growth. *Cell Cycle*. 2007;6:2323-2326.
54. Kyosseva SV. The role of the extracellular signal-regulated kinase pathway in cerebellar abnormalities in schizophrenia. *Cerebellum*. 2004;3:94-99.
55. Jee YH, Sowada N, Markello TC, Rezvani I, Borck G, Baron J. BRF1 mutations in a family with growth failure, markedly delayed bone age, and central nervous system anomalies. *Clin Genet*. 2017;91:739-747.
56. Ferguson SM, Brasnjo G, Hayashi M, et al. A selective activity-dependent requirement for dynamin 1 in synaptic vesicle endocytosis. *Science*. 2007;316:570-574.
57. Kelly BL, Vassar R, Ferreira A. Beta-amyloid-induced dynamin 1 depletion in hippocampal neurons. A potential mechanism for early cognitive decline in Alzheimer disease. *J Biol Chem*. 2005;280:36:1746-1753.
58. Vallortigara J, Rangarajan S, Whitfield D, et al. Dynamin1 concentration in the prefrontal cortex is associated with cognitive impairment in Lewy body dementia. *PLoS One*. 2014;9:e108.
59. Fa M, Staniszewski A, Saeed F, Francis YI, Arancio O. Dynamin 1 is required for memory formation. *PLoS One*. 2014;9:e91954.
60. Wefel JS, Vardy J, Ahles T, Schagen SB. International cognition and cancer task force recommendations to harmonise studies of cognitive function in patients with cancer. *Lancet Oncol*. 2011;12:703-708.
61. Deprez S, Kesler SR, Saykin AJ, Silverman DHS, de Ruiter MB, McDonald BC. International cognition and cancer task force recommendations for neuroimaging methods in the study of cognitive impairment in non-CNS cancer patients. *J Natl Cancer Inst*. 2018;110:223-231.
62. Fan F, Funk L, Lou X. Dynamin 1- and 3-mediated endocytosis is essential for the development of a large central synapse in vivo. *J Neurosci*. 2016;36:6097-6115.
63. Greene C, Campbell M. Tight junction modulation of the blood brain barrier: CNS delivery of small molecules. *Tissue Barriers*. 2016;4:e1138017.
64. Gunzel D, Yu AS. Claudins and the modulation of tight junction permeability. *Physiol Rev*. 2013;93:525-569.
65. Fauquette W, Amourette C, Dehouck MP, Diserbo M. Radiation-induced blood-brain barrier damages: an in vitro study. *Brain Res*. 2012;1433:114-126.
66. Yuan H, Gaber MW, McColgan T, Naimark MD, Kiani MF, Merchant TE. Radiation-induced permeability and leukocyte adhesion in the rat blood-brain barrier: modulation with anti-ICAM-1 antibodies. *Brain Res*. 2003;969:59-69.
67. Craver BM, Acharya MM, Allen BD, et al. 3D surface analysis of hippocampal microvasculature in the irradiated brain. *Environ Mol Mutagen*. 2016;57:341-349.

68. Balbuena P, Li W, Ehrlich M. Assessments of tight junction proteins occludin, claudin 5 and scaffold proteins ZO1 and ZO2 in endothelial cells of the rat blood-brain barrier: cellular responses to neurotoxicants malathion and lead acetate. *Neurotoxicology*. 2011;32:58-67.
69. Liu C, Wu J, Zou MH. Activation of AMP-activated protein kinase alleviates high-glucose-induced dysfunction of brain microvascular endothelial cell tight-junction dynamics. *Free Radic Biol Med*. 2012;53:1213-1221.
70. Zhong X, Luo C, Deng M, Zhao M. Scutellarin-treated exosomes increase claudin 5, occludin and ZO1 expression in rat brain microvascular endothelial cells. *Exp Ther Med*. 2019;18:33-40.
71. Liang T, Ju H, Zhou Y, Yang Y, Shi Y, Fang H. Inhibition of glycogen synthase kinase 3beta improves cognitive function in aged mice by upregulating claudin presences in cerebral endothelial cells. *Acta Biochim Biophys Sin (Shanghai)*. 2020;52:363-370.
72. Dearborn JL, Urrutia VC, Zeiler SR. Stroke and cancer- a complicated relationship. *J Neurol Transl Neurosci*. 2014;2:1039.
73. Zaorsky NG, Zhang Y, Tehelebi LT, Mackley HB, Chinchilli VM, Zacharia BE. Stroke among cancer patients. *Nat Commun*. Nov 15 2019;10:5172.
74. Lochhead JJ, Yang J, Ronaldson PT, Davis TP. Structure, function, and regulation of the blood-brain barrier tight junction in central nervous system disorders. *Front Physiol*. 2020;11:914.
75. Starobova H, Mueller A, Deuis JR, Carter DA, Vetter I. Inflammatory and neuropathic gene expression signatures of chemotherapy-induced neuropathy induced by vincristine, cisplatin, and oxaliplatin in C57BL/6J mice. *J Pain*. 2020;21:182-194.
76. Shenoy A, Belugali Nataraj N, Perry G, et al. Proteomic patterns associated with response to breast cancer neoadjuvant treatment. *Mol Syst Biol*. 2020;16:e9443.
77. Brown T, McElroy T, Simmons P, et al. Cognitive impairment resulting from treatment with docetaxel, doxorubicin, and cyclophosphamide. *Brain Res*. 2021;1760:147397.
78. Branca JJV, Maresca M, Morucci G, et al. Oxaliplatin-induced blood brain barrier loosening: a new point of view on chemotherapy-induced neurotoxicity. *Oncotarget*. 2018;9:23426-23438.